

The Role of LC3-Associated Phagocytosis Inhibits the Inflammatory Response in *Aspergillus fumigatus* Keratitis

Junjie Luan,¹ Ziyue Zhang,^{1,2} Qian Wang,¹ Cui Li,¹ Hao Zhang,¹ Yingxue Zhang,³ Xudong Peng,¹ Guiqiu Zhao,¹ and Jing Lin¹

¹Department of Ophthalmology, The Affiliated Hospital of Qingdao University, Qingdao, Shandong Province, China

²Department of Ophthalmology, Qingdao Central Hospital, Qingdao, Shandong Province, China

³Department of Biochemistry, Microbiology, and Immunology, Wayne State University School of Medicine, Detroit, Michigan, United States

Correspondence: Jing Lin and Guiqiu Zhao, Department of Ophthalmology, The Affiliated Hospital of Qingdao University, NO. 16 Jiangsu Road, Qingdao, Shandong Province 266000, China; yankelinjing@126.com and zhaoguiqiu_good@126.com.

Junjie Luan and Ziyue Zhang contributed equally to this study and should be considered co-first authors.

Received: May 27, 2023

Accepted: April 18, 2024

Published: July 2, 2024

Citation: Luan J, Zhang Z, Wang Q, et al. The role of LC3-associated phagocytosis inhibits the inflammatory response in *Aspergillus fumigatus* keratitis. *Invest Ophthalmol Vis Sci*. 2024;65(8):4. <https://doi.org/10.1167/iovs.65.8.4>

PURPOSE. The purpose of this study was to investigate the role and mechanism of microtubule-associated protein light chain-3 (LC3)-associated phagocytosis (LAP) in the immune response to *Aspergillus fumigatus* (*A. fumigatus*) keratitis.

METHODS. The formation of single-membrane phagosomes was visualized in the corneas of healthy or *A. fumigatus*-infected humans and C57BL/6 mice using transmission electron microscopy (TEM). Rubicon siRNA (si-Rubicon) was used to block Rubicon expression. RAW 264.7 cells or mice corneas were infected with *A. fumigatus* with or without pretreatment of si-Rubicon and scrambled siRNA. RAW 264.7 cells were pretreated with Dectin-1 antibody or Dectin-1 overexpressed plasmid and then stimulated with *A. fumigatus*. Flow cytometry was used to label macrophages in normal and infected corneas of mice. In mice with *A. fumigatus* keratitis, the severity of the disease was assessed using clinical scores. We used lentiviral technology to transfer GV348-Ubi-GFP-LC3-II-SV40-Puro Lentivirus into the mouse cornea. The GFP-LC3 fusion protein was visualized in corneal slices using a fluorescence microscope. We detected the mRNA and protein expressions of the inflammatory factors IL-6, IL-1 β , and IL-10 using real-time PCR (RT-PCR) and ELISA. We detected the expression of LAP-related proteins Rubicon, ATG-7, Beclin-1, and LC3-II using Western blot or immunofluorescence.

RESULTS. Accumulation of single-membrane phagosomes within macrophages was observed in the corneas of patients and mice with *A. fumigatus* keratitis using TEM. Flow cytometry (FCM) analysis results show that the number of macrophages in the cornea of mice significantly increases after infection with *A. fumigatus*. LAP-related proteins were significantly elevated in the corneas of mice and RAW 264.7 cells after infection with *A. fumigatus*. The si-Rubicon treatment elevated the clinical score of mice. In *A. fumigatus* keratitis mice, the si-Rubicon treated group showed significantly higher expression of IL-6 and IL-1 β and lower expression of IL-10 and LC3-II compared to the control group. In RAW 264.7 cells, treatment with the Dectin-1 overexpressed plasmid upregulated the expression of LAP-related proteins, a process that was significantly inhibited by the Dectin-1 antibody.

CONCLUSIONS. LAP participates in the anti-inflammatory immune process of fungal keratitis (FK) and exerts an anti-inflammatory effect. LAP is regulated through the Dectin-1 signaling pathway in *A. fumigatus* keratitis.

Keywords: light chain-3 (LC3)-associated phagocytosis (LAP), *Aspergillus fumigatus* (*A. fumigatus*), keratitis, anti-inflammation, immunity

Fungal keratitis (FK), a corneal disease with a high rate of blindness, is caused by pathogenic fungi. In developing countries, *Aspergillus fumigatus* (*A. fumigatus*) remains one of the main pathogens of FK.^{1,2} When *A. fumigatus* invades, pathogen-associated molecular patterns (PAMPs) on the *A. fumigatus* cell wall can be recognized by pattern recognition receptors (PRRs) of the cornea, initiating the innate immune response against the fungal pathogens.³ This

process mediates the release of chemokines and inflammatory factors.⁴ Furthermore, macrophages are recruited to the infected cornea to expedite the elimination of the fungus.⁵ Fungal invasion can lead to corneal edema, ulceration, and proliferative scarring, which are significant causes of impaired vision and blindness. Therefore, effective removal of the fungus is vital to protect the cornea.

Microtubule-associated protein light chain 3 (LC3)-associated phagocytosis (LAP) is a noncanonical autophagy process.^{6,7} Studies have found that LAP plays a crucial role in fungus removal,⁸ and this process is dependent on members of the canonical autophagy pathway, including Beclin-1, ATG-7, and LC3-II.⁹ LC3, a crucial protein in both LAP and the canonical autophagy process, binds with phosphatidylethanolamine in the cytoplasm to generate LC3-II.¹⁰ The lipidated form of LC3 is incorporated into the double membrane of the autophagosome, facilitating its maturation and formation. In contrast to the double-layer membrane structure of conventional autophagosomes, phagocytic vesicles associated with LAP exhibit single-layered membrane structures.¹⁰ Compared with canonical autophagy, the pre-initiation complex (comprising ULK1/2, FIP200, and Atg13) is dispensable for LAP, whereas the class III PI3K complex is required.⁷ Activation of PRRs by PAMPs can trigger the recruitment of autophagy-related proteins, the formation of the class III PI3K complex, and the rapid recruitment of LC3 to a singular phagosomal membrane. This process facilitates the expedited maturation of LAP-related phagocytic vesicles.¹¹ In comparison to autophagosomes, phagosomes associated with LAP exhibit a higher propensity to promptly merge with lysosomes, thereby expediting fungal elimination and enhancing the efficiency of the body's immune response.^{9,10} Recently, it has been revealed that the autophagy protein Rubicon, characterized by an RUN domain and its interaction with Beclin-1, as well as its cysteine-rich nature, is essential for the initiation of LAP but not for autophagy induction.^{9,12,13}

Recently, the role of LAP in the clearance of fungal pathogens has been demonstrated.¹⁴ LAP plays a significant role in the antifungal host defense mechanism of *A. fumigatus*.¹⁵ It has been demonstrated that deficiencies in LAP exacerbate susceptibility to fungi and increase the expression of pro-inflammatory factors, while reducing the expression of anti-inflammatory factors.¹⁶ For instance, in the mouse model of *A. fumigatus* pneumonia, LAP-deficient mice exhibited an augmented inflammatory response, reduced spore clearance, and elevated expression of pro-inflammatory cytokines.^{17–19} Studies have indicated that patients with Dectin-1^{-/-} show decreased recruitment of LC3-II to *Aspergillus*-containing phagosomes.^{20,21} Additionally, Dectin-1-deficient cells are even less likely to produce lipidated LC3 when exposed to whole yeast or β -glucan.^{22,23}

We have previously demonstrated in animal models that the conventional autophagic pathway may play a potential role in corneas following *A. fumigatus* infection. This pathway may exhibit a positive correlation with the severity of keratitis and associated pathological alterations.²⁴ However, the role of LAP in *A. fumigatus* keratitis remains unexplored.

In this study, we first found the presence of single-membrane phagosomes in the corneal stroma following infection with *A. fumigatus*. Furthermore, we demonstrated that LAP plays a crucial role in the immune response to *A. fumigatus* keratitis. Moreover, our research revealed that *A. fumigatus* modulated LAP via the Dectin-1 pathway. Our study may provide a therapeutic solution for *A. fumigatus* keratitis.

MATERIALS AND METHODS

Corneal Samples of Patients With FK

Twenty patients (20 eyes) with *A. fumigatus* keratitis underwent penetrating keratoplasty, and corneas with lesions

were collected. *A. fumigatus* keratitis was diagnosed by culture of cornea scrapings. Twenty healthy donor corneas were used for corneal transplantation, and the remaining peripheral corneal tissues were collected as control groups. The corneas were preserved in 2.5% glutaraldehyde (Solarbio, Beijing, China) for 2 minutes in preparation for examination by transmission electron microscopy (TEM). The study protocol adhered to the provisions of the Declaration of Helsinki. The human cornea tissue providers all signed informed consent forms for specimen processing. The experiment was approved by the Affiliated Hospital of Qingdao University's ethics committee (No. QYFY WZLL 27589).

A. fumigatus Culture

The standard *A. fumigatus* strain 3.0772 was purchased from the China Microbiological Culture Preservation Management Center (Beijing, China). The conidia were cultured for 2 days at 37°C and 200 rpm in Sabouraud liquid medium. The culture medium was washed with PBS containing 0.1% Tween 20. We obtained activated hyphae and inactivated hyphae, which were sterilized in 70% ethanol overnight. The final concentration of the harvested *Aspergillus* mycelia was adjusted to 1×10^8 CFU/mL. Conidia on the surface of the medium were collected and adjusted to a final concentration of 3×10^7 conidia μL^{-1} .

Mice Model of FK

Eight-week-old female C57BL/6 mice were purchased from Sibeifu Laboratory Animal Co. Ltd. (Beijing, China) and were treated in accordance with the ARVO Statement for the Use of Animals in Ophthalmic and Visual Research. The procedures followed the guidelines of the Animal Care and Use Committee of the Affiliated Hospital of Qingdao University (No. QYFY WZLL 27589). The mouse model of FK was established based on previous studies.² A slit lamp microscope was used to observe all mice corneas to obtain the clinical scores in accordance with a 12-point scoring system, as demonstrated previously.² Mice corneas were collected at the indicated times after infection. The corneas were used for real-time PCR (RT-PCR), electron microscopy, Western blot, ELISA, and flow cytometry. The mice eyeballs were harvested for immunohistofluorescence staining (IFS).

A. fumigatus Stimulation of RAW 264.7 Cells

RAW 264.7 cells (Chinese Academy of Sciences, China) were cultivated following the methods previously described.⁴ When cells reached approximately 80% confluence, they were incubated with *A. fumigatus* hyphae (5×10^6 CFU/mL) in 12-well and 6-well plates for 0, 12, and 24 hours for RT-PCR, immunofluorescence, and Western blot.

Real-Time PCR

Total RNA from corneas and cells was measured using RNAiso plus reagent (TaKaRa, Dalian, China), and RT-PCR was conducted based on previous experimental studies.⁵ The primer sequences are shown in the [Table](#).

Western Blot

Total protein was extracted from corneas ($n = 6$ mice/group) or RAW 264.7 cells using a lysis buffer (RIPA: PMSF:

TABLE. Target Gene Primer Sequence

Gene	GenBank No.	Primer Sequence (5'-3')
Mouse β -actin	NM_007393.5	F: GATTACTGCTCTGGCTCCTAGC R: GACTCATCGTACTCCTGCTTGC
Mouse IL-1 β	NM_008361.4	F: CGCAGCAGCACATCAACAAGAGC R: TGTCTCATCCTGGAAGGTCCACG
Mouse IL-6	NM_001314054.1	F: TGATGGATGCTACCAAAGTGG R: TGTGACTCCAGCTTATCTCTTGG
Mouse IL-10	NM_010548.2	F: TGCTAACCCGACTCCTTAATGCA R: TTCTCACCCAGGGAATTCAA

F, forward; R, reverse.

phosphatase inhibitor = 98:1:1). Protein concentration was measured using the BCA assay (Solarbio). The proteins were separated on a 12% SDS-PAGE gel and transferred onto a PVDF membrane (Solarbio). After incubation in blocking buffer (Solarbio) for 2 hours, the blots were incubated overnight with the primary antibodies against β -actin (1:5000; Elabscience, Wuhan, China), β -tubulin (1:1000; Elabscience), Rubicon (1:1000; Abcam, Cambridge, MA, USA), ATG-7 (1:1000; Abcam), Beclin-1 (1:1000; Abcam), and LC3-II (1:1000; Abcam) at 4°C. The next day, they were incubated with secondary antibodies for 2 hours. Protein bands were visualized using chemiluminescence (ECL; Thermo Fisher Scientific, USA).

Label LC3-II Through Lentiviral

Corneas of mice were transfected with GV348-Ubi-GFP-LC3-II-SV40-Puro Lentivirus (10^8 TU/mL; Jikai Genetic Chemical Technology Co., Ltd., Shanghai, China). In short, mice were abdominally anesthetized with 8% chloral hydrate (0.4 mL/kg). Then, 1.5 μ L of lentivirus was injected into the right corneal stroma under the stereoscopic microscope once daily for 7 days. Subsequently, we established the model of *A. fumigatus* keratitis after achieving stable transfection. The left eyes were blank control. Eyeballs of mice were harvested at 3 days post-infection (pi). Mice eyeballs from different groups were embedded in optimal cutting temperature (OCT; Sakura Finetek USA, Inc., USA) and frozen in liquid nitrogen. Eyeballs were cut transversely to yield 10 μ m slices. The GFP-LC3 fusion protein was visualized in corneal slices under a fluorescence microscope (Leica Microsystems).

Transmission Electron Microscopy

Corneas from healthy donors, patients with FK, and mice in different groups were fixed with 2.5% glutaraldehyde at 4°C for 12 hours. Subsequently, the corneas were observed using TEM.

Immunofluorescence Assays

RAW 264.7 cells were seeded on poly-L-lysine-coated slips in 24-well plates for 12 hours. Then, RAW 264.7 cells were treated with *A. fumigatus* hyphae for 12 hours. After blocking with goat serum (1:100; Abcam, Cambridge, UK), the cells were incubated with anti-mouse Rubicon, ATG-7, and Beclin-1 antibodies (1:200; Santa Cruz, CA, USA) for 12 hours, and then incubated with FITC-conjugated goat anti-rabbit antibody (1:200; Abcam) for 1 hour. Analysis of the proportion of Rubicon, ATG-7, and Beclin-1 positive

cells was determined in immunofluorescence assays.²⁵ We observed and photographed 24 fields of view of each poly-L-lysine-coated slip under a fluorescence microscope (Zeiss Axio Vert, 400 \times).

Immunohistofluorescence Staining

Eyeballs of mice were harvested at 3 days pi. Slices of cornea were prepared as previously described. Slices of cornea were stained with anti-mouse anti-F4/80 antibodies (10 μ g/mL) overnight at 4°C. The slices were stained with FITC-conjugated goat anti-rabbit antibody (Abcam, 1:200) for 1 hour. Nuclei were counterstained with DAPI (Solarbio), and slides were imaged under a fluorescence microscope at 400 \times magnification.

Enzyme-Linked Immunosorbent Assay

We performed euthanasia on mice using the cervical dislocation method 3 days after infection. Then, the corneas of the mice ($n = 5$ /group/time) were removed, ground, and homogenized in 500 μ L of PBS containing 0.1% Tween 20 and protease inhibitor (Solarbio, Beijing, China). The supernatant was prepared by centrifugation (5000 g) for 10 minutes at 4°C. ELISA was performed according to the manufacturer's instructions (Elabscience, Wuhan, China). Using IL-1 β , IL-6, and IL-10 ELISA kits, the amount of undiluted supernatant was measured.

Si-Rubicon Pretreatment of the Cornea and RAW 264.7 Cells

The si-Rubicon was used to block Rubicon expression. The right eyes were treated with si-Rubicon (10 nM; Ribobio, Guangzhou, China) or scrambled siRNA (10 nM; Ribobio, Guangzhou, China). The left eye was untreated as a blank control. The si-Rubicon or scrambled siRNA was injected into the subconjunctival of mice 1 day before infection and once on the day of infection. The corneas of mice were collected after 1, 3, and 5 days pi. RAW 264.7 cells were seeded into 12-well cell culture plates. RAW 264.7 cells were pretreated with si-Rubicon (50 nM) or scrambled siRNA (50 nM) for 24 hours until the cells reached 80% to 90% confluency and then stimulated by *A. fumigatus* for 12 hours. Corneas and cells were analyzed by RT-PCR.

Dectin-1 Polyclonal Antibody Pretreatment

RAW 264.7 cells were seeded into 6-well plates until reaching 80% confluency. RAW 264.7 cells were treated with 25 μ g/mL

of Dectin-1 polyclonal antibody (R&D Systems, USA) at 37°C for 1 hour, and then incubated with *A. fumigatus* hyphae (5×10^6 CFU/mL) for 24 hours. RAW 264.7 cells were collected for Western blot analysis to assess the protein levels of Rubicon, Beclin-1, ATG-7, and LC3-II.

Dectin-1 Overexpressed Plasmids

Construction of plasmid (Jikai Genetic Chemical Technology Co., Ltd., Shanghai, China) and cell transfection. RAW 264.7 transfection experiments were conducted following the protocol for the transfection reagent Lipofectamine 3000 (Thermo Fisher Scientific, Waltham, MA, USA). The reagent was diluted and mixed with OPTI-MEM medium. Next, we prepared the Dectin-1 DNA premix by diluting 1 µg of Dectin-1 DNA with 50 µL OPTI-MEM medium, and then added the P3000 reagent to achieve the desired concentration (2 µL/µg). Subsequently, the diluted Dectin-1 DNA was added to the diluted reagent (1:1) and then incubated for 15 minutes to obtain Dectin-1 DNA-lipid complexes. Dectin-1 overexpressing plasmids were established. RAW 264.7 cells were incubated with the prepared complexes in 6-well plates for 48 hours. Subsequently, the cells were collected for Western blot analysis to assess the levels of Rubicon and LC3-II proteins.

Flow Cytometry Analysis

Mice corneas ($n = 5$ /group) were harvested at 3 days pi. Normal corneas or infected corneas were lysed into single cells using liberase (Roche, Basel, Switzerland). The method steps were based on our previous research.⁴ The number of macrophages in the cornea labeled with fluorescent antibodies was estimated by a Beckman flow cytometer (Krefeld, Germany) and analyzed with FlowJo X software. The staining dyes and antibodies used are as follows: CD45-PERCP Cy5.5 (1:200; Biolegend, San Diego, CA, USA) and F4/80-PE Cy7 (1:200; Biolegend, San Diego, CA, USA).

Statistical Analyses

GraphPad version 7.0 (San Diego, CA, USA) and ImageJ (Bethesda, MD, USA) were used to analyze data. Data were presented as median or mean \pm SEM. To compare the differences between the two groups, the significance of the two groups was determined using an unpaired, two-tailed Student's *t*-test, whereas the comparison among 3 or more groups was evaluated by 1-way ANOVA. The $P < 0.05$ ($*P < 0.05$, $**P < 0.01$, and $***P < 0.001$) was considered significant. All experiments were repeated at least three times.

RESULTS

Single-Membrane Phagosome Formation in Corneas of Patients With FK and Mice Models of FK

The presence of single-membrane phagosomes is a significant indicator of LAP. TEM images revealed the absence of single-membrane phagosomes in the corneal stroma of both normal humans (Fig. 1A) and mice (Fig. 1D). Conversely, single-membrane phagosomes were observed in macrophages within the corneal stroma of both *A. fumigatus*-infected humans (Figs. 1B, 1C) and mice (Figs. 1E, 1F). A mouse model of *A. fumigatus* keratitis

was established. The slit lamp images and clinical scores clearly indicated increased disease severity at 3 days pi (Figs. 1G, 1H). Flow cytometry (FCM) analysis revealed a significant increase in the number of macrophages in the corneas of mice at 3 days pi compared to the control group (Figs. 1I–K).

Expression of LAP-Related Proteins in Corneas of Mice With *A. fumigatus* Keratitis

In order to further explore the expression of LAP-related proteins in the corneas of mice after fungal infection, we established the mouse model of *A. fumigatus* keratitis. Western blot and immunofluorescence were used to detect the expression of LAP-related proteins. Compared with the normal group, *A. fumigatus* infection increased the expression of Rubicon (Fig. 2A), ATG-7 (Fig. 2C), and Beclin-1 (Fig. 2E) in the corneas of mice at 1 day pi, and reached a peak at 3 days pi. The protein level of LC3-II (Fig. 2G) gradually increased at 1, 3, and 5 days pi. Furthermore, mouse corneas were transfected with GV348-Ubi-GFP-LC3-II-SV40-Puro lentivirus, and subsequently, the mice *A. fumigatus* keratitis model was established. Immunostaining demonstrated that significantly higher levels of GFP-LC3 accumulated in *A. fumigatus*-infected corneas (Fig. 2J) compared to normal mice corneas (Fig. 2I).

Anti-Inflammatory Effect of LAP in *A. fumigatus* Keratitis

We interfered with the expression of Rubicon through si-Rubicon. The expression level of Rubicon mRNA was used to assess the efficiency of si-Rubicon interference in RAW 264.7 cells. Compared to the scrambled siRNA pretreated group, the expression of Rubicon mRNA was significantly reduced in the si-Rubicon pretreated group (Fig. 3A). Western blot results showed that the protein expression of Rubicon (Fig. 3B) and LC3-II (Fig. 3D) were reduced in the si-Rubicon pretreated groups at 3 days pi. The slit lamp photographs of mouse corneas showed that treatment with si-Rubicon significantly increased clinical scores (Figs. 3F, 3G). Results of RT-PCR showed that the relative mRNA levels of IL-6 (Fig. 3H) and IL-1 β (Fig. 3I) were elevated in corneas after si-Rubicon treatment compared with the infected group at 3 days pi. Compared with the infected group, the mRNA level of IL-10 (Fig. 3J) was decreased in corneas treated with si-Rubicon at 3 days pi. Consistent with the results of RT-PCR, we observed that si-Rubicon treatment enhanced the protein levels of IL-6 (Fig. 3K) and IL-1 β (Fig. 3L) in the corneas, while also decreasing the protein level of IL-10 (Fig. 3M).

The Mechanism of Fungal Antigen-Induced LAP Production in *A. fumigatus* Keratitis

We examined the expression of LAP-related protein in the RAW 264.7 cells after stimulation with *A. fumigatus*. The protein levels of Rubicon (Figs. 4A, 4B), ATG-7 (Figs. 4C, 4D), Beclin-1 (Figs. 4E, 4F), and LC3-II (Figs. 4G, 4H) increased compared to the normal group. In addition, immunostaining demonstrated that Rubicon (Figs. 4I, 4J), ATG-7 (Figs. 4K, 4L), and Beclin-1 (Figs. 4M, 4N) increased in RAW 264.7 cells after *A. fumigatus* stimulation. We then explored the mechanism of fungal antigen-induced LAP in *A. fumigatus* keratitis. RAW 264.7 cells were treated

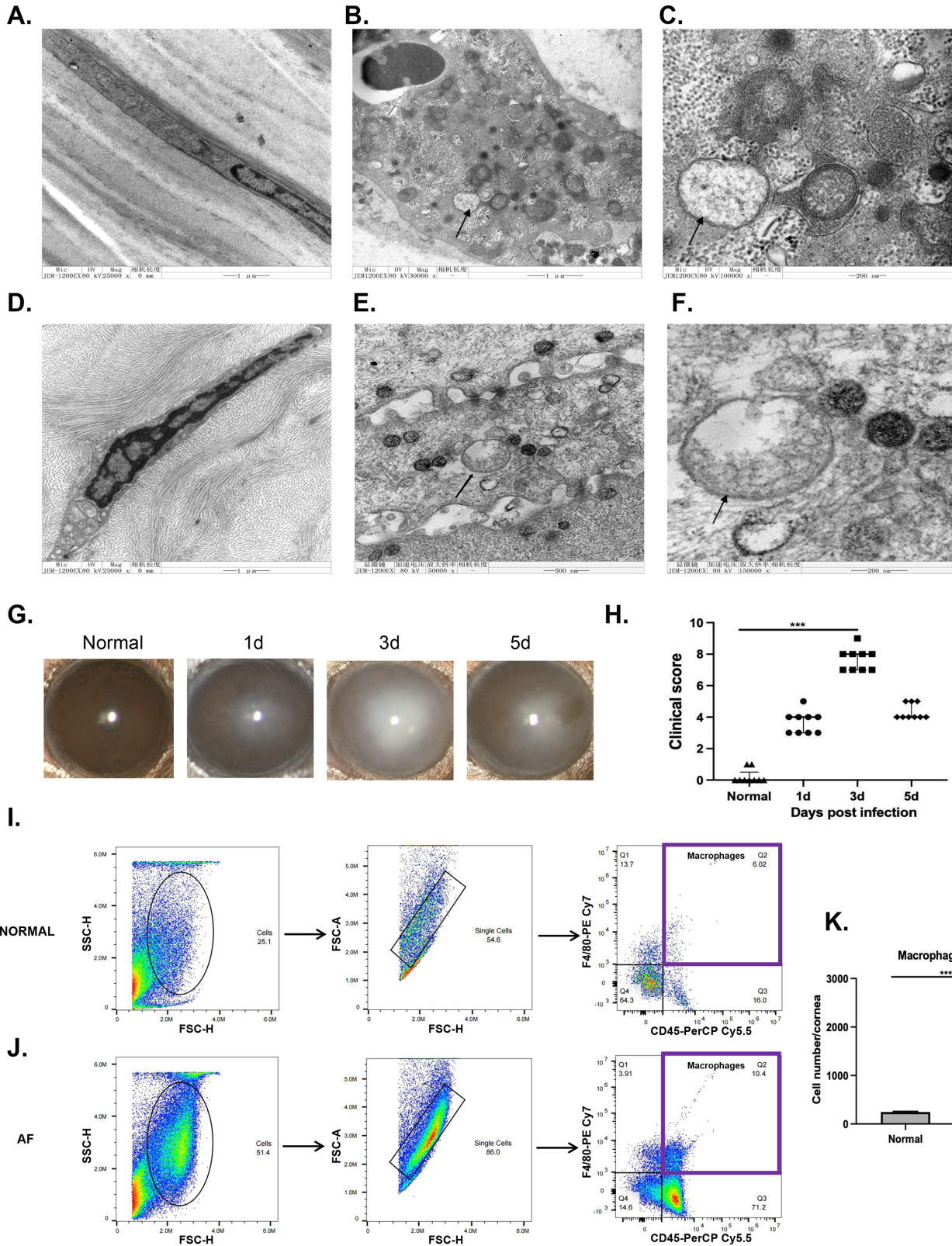


FIGURE 1. Single-membrane phagosomes formation in patients and mice with *A. fumigatus* keratitis. TEM images showed the corneal stroma in both healthy humans (A) and mice (D). Additionally, TEM images illustrated macrophages within the corneal stroma of humans infected with *A. fumigatus* (B, C). Similar images were captured of the corneal stroma in mice at 3 days pi. Black arrows highlight single-membrane phagosomes in the macrophages (B, C, E, F). Slit lamp images of mice corneas (G) were obtained at 1, 3, and 5 days pi., showing a significant increase in clinical scores at 3 days pi (H). Normal and *A. fumigatus*-infected corneas were collected for FCM analysis. Gating on single cells, CD45+ cells were immune cells, and CD45+ F4/80+ cells were macrophages. Representative flow cytometric plots (I, J) and data showed the number of macrophages in corneas (K). Clinical scores were analyzed using the Mann-Whitney *U* test. ****P* < 0.001.

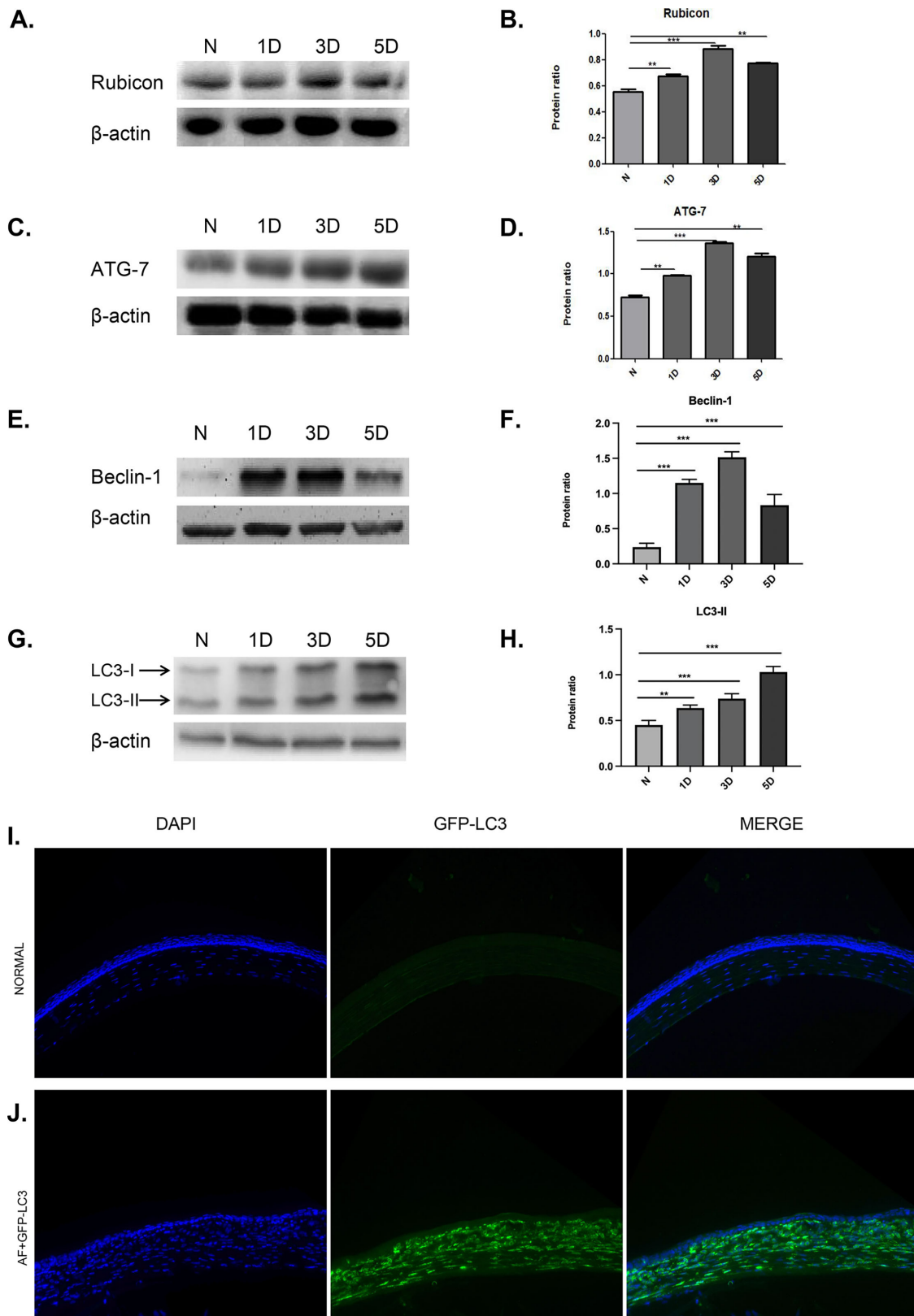


FIGURE 2. Expression of LAP-related protein in *A. fumigatus* keratitis mouse models. β -actin is a housekeeping protein whose stable expression is relatively constant in each group and is used to an internal control for protein expression normalization in Western blotting. Rubicon (A, B), ATG-7 (C, D), Beclin-1 (E, F), and LC3-II (G, H) protein levels were significantly increased at 1, 3, and 5 days after infection ($n = 6$ mice/group). Corneas of mice were transfected with GV348-Ubi-GFP-LC3-II-SV40-Puro Lentivirus. The GFP-LC3 fusion protein (green) was visualized in corneal slices at a magnification of 400 \times using a fluorescence microscope on the third day pi ($n = 6$ mice/group). The expression of LC3 was significantly higher in mice corneas at 3 days pi (I, J). All data were mean \pm SEM. * $P < 0.05$; ** $P < 0.01$; *** $P < 0.001$.

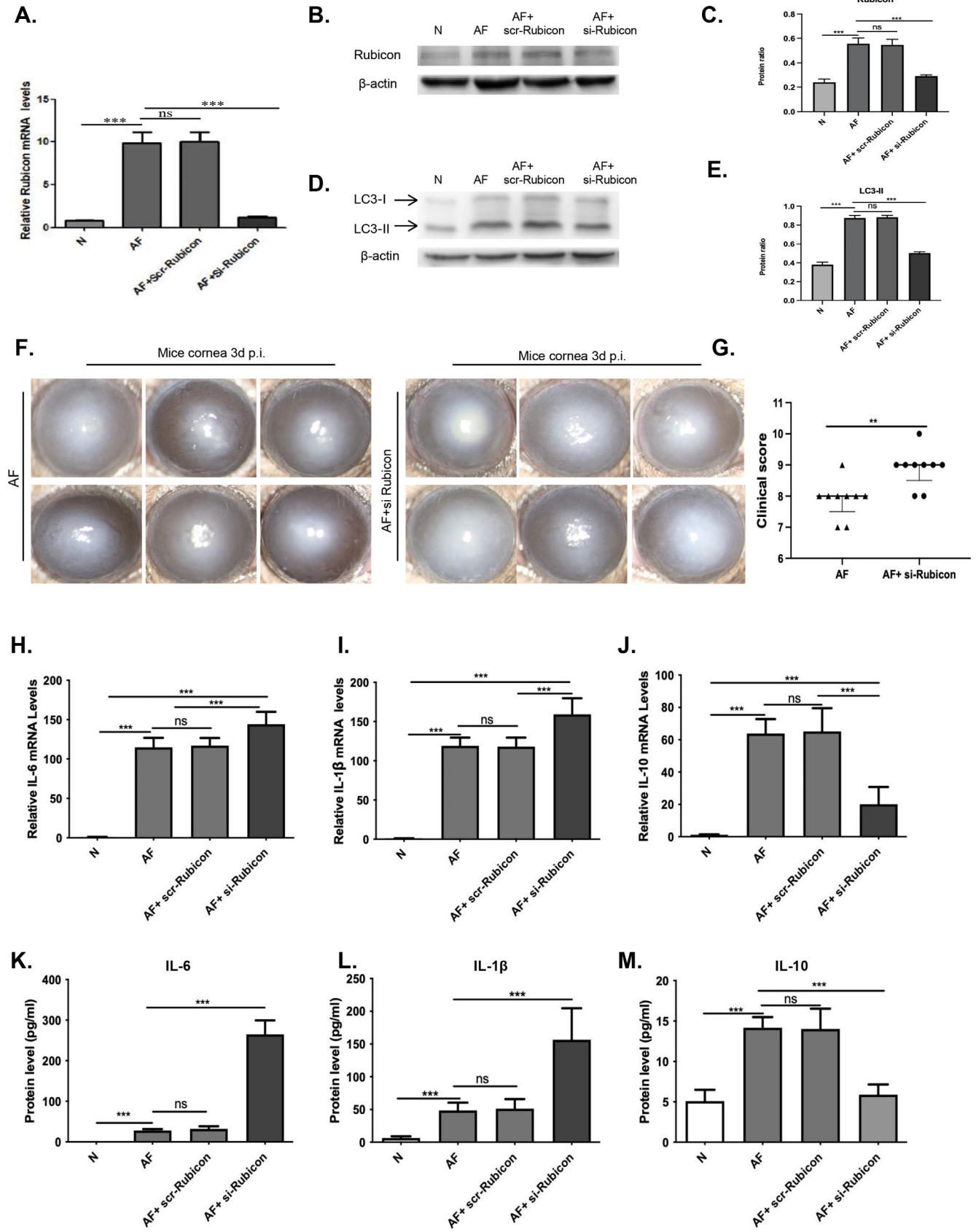


FIGURE 3. The effect of LAP on the inflammatory response. RAW 264.7 cells were pretreated with si-Rubicon or scrambled siRNA for 24 hours, and then incubated with *A. fumigatus* for 8 or 24 hours. RT-PCR results showed that the expression level of Rubicon mRNA was significantly reduced in RAW 264.7 cells treated with si-Rubicon (A). Corneas of mice were pretreated with si-Rubicon or scrambled siRNA for 2 days and then stimulated with *A. fumigatus*. Western blot results and grayscale analysis demonstrated that the protein expression levels of Rubicon (B, C) and LC3-II (D, E) were significantly reduced in the si-Rubicon treatment groups. Clinical scores were signifi-

cantly higher in the si-Rubicon treatment groups (F, G). The mRNA and protein levels of IL-6 (H, I, J, K), IL-1 β (I, J, K, L), and IL-10 (J, K, L, M) in the corneas of mice after si-Rubicon treatment at 3 days pi. Clinical scores were analyzed using the Mann-Whitney *U* test. All data were mean \pm SEM (ns = no significance; **P* < 0.05; ***P* < 0.01; ****P* < 0.001.)

with Dectin-1 polyclonal antibody or Dectin-1 overexpressed plasmids, and then stimulated by *A. fumigatus*. The Western blot results indicated that the expression of Rubicon (Figs. 4O, 4R), ATG-7 (Figs. 4P, 4S), Beclin-1 (Figs. 4Q, 4T), and LC3-II (Figs. 4U, 4X) were decreased when pretreated

with Dectin-1 antibody compared to the infection group. In addition, Dectin-1 overexpression plasmid pretreatment increased LC3-II (Figs. 4V, 4Y) and Rubicon (Figs. 4W, 4Z) protein expression levels compared with the simple infection group.

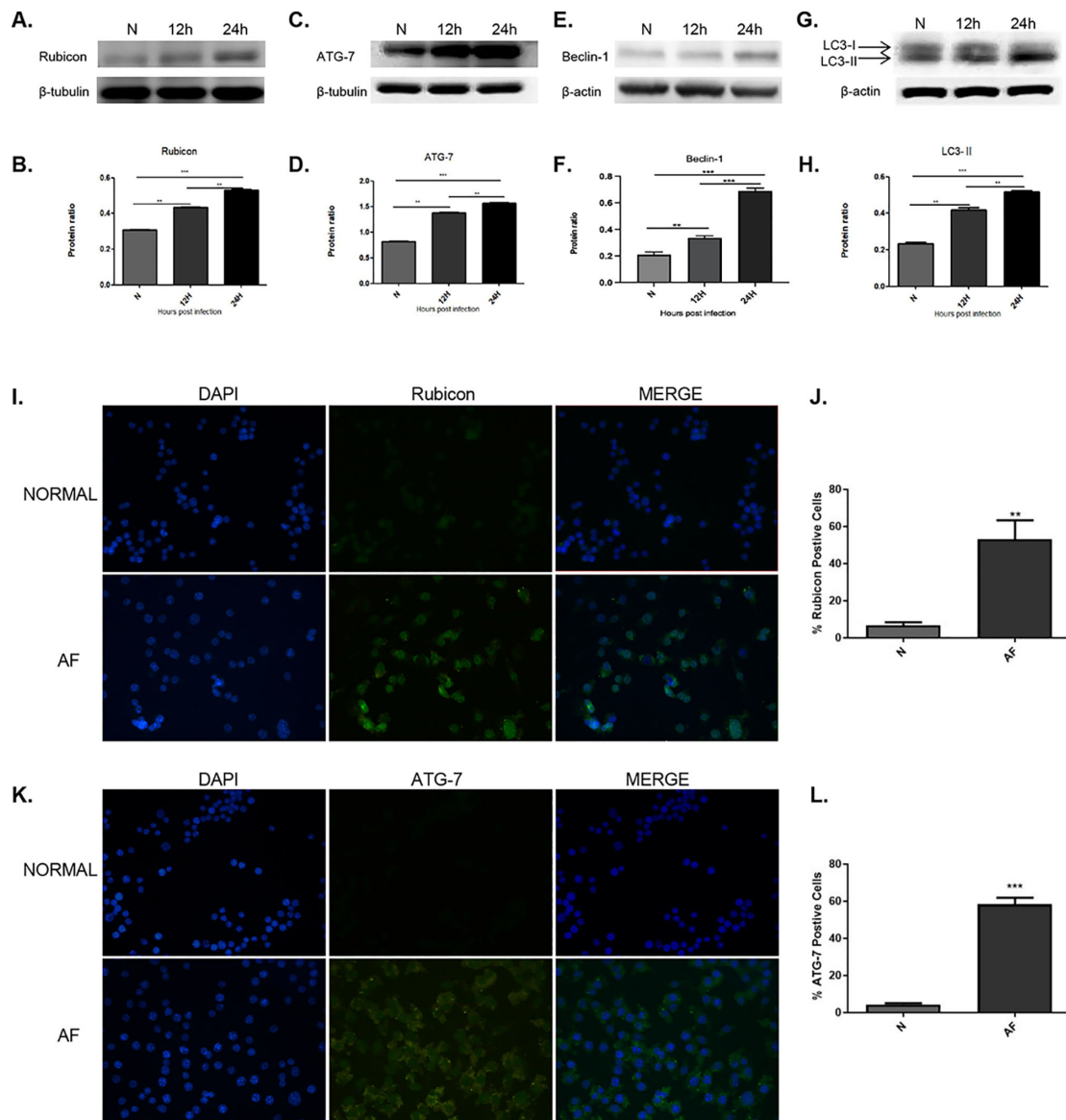


FIGURE 4. Dectin-1 regulates the expression of Lap-related proteins in *A. fumigatus* keratitis. RAW 264.7 cells were incubated with *A. fumigatus* hyphae for 12 and 24 hours. Western blot results showed that the protein expression levels of Rubicon (A, B), ATG-7 (C, D), Beclin-1 (E, F), and LC3-II (G, H) were significantly increased after stimulation by *A. fumigatus*. Immunofluorescence images showed the expression of Rubicon (I), ATG-7 (K), and Beclin-1 (M) in *A. fumigatus*-infected RAW 264.7 cells. Proportion of Rubicon (J), ATG-7 (L), and Beclin-1 (N) positive cells. Green = Rubicon, ATG-7, Beclin-1 (FITC); blue = nucleus (DAPI). RAW 264.7 cells were treated with Dectin-1 polyclonal antibody or Dectin-1 overexpressed plasmids, and then incubated with *A. fumigatus* hyphae for 24 hours. The protein levels of Rubicon (O, P, Q, R), ATG-7 (P, Q, R, S), Beclin-1 (Q, R, S, T), and LC3-II (U, V, W, X) were significantly decreased in the Dectin-1 antibody pretreated groups. Conversely, the protein levels of LC3-II (V, W, X, Y) and Rubicon (W, X, Y, Z) were significantly increased in the groups pretreated with the Dectin-1 overexpression plasmid. All data were mean \pm SEM (ns = no significance; **P* < 0.05; ***P* < 0.01; ****P* < 0.001.) Magnification, 400 \times (I, K, M).

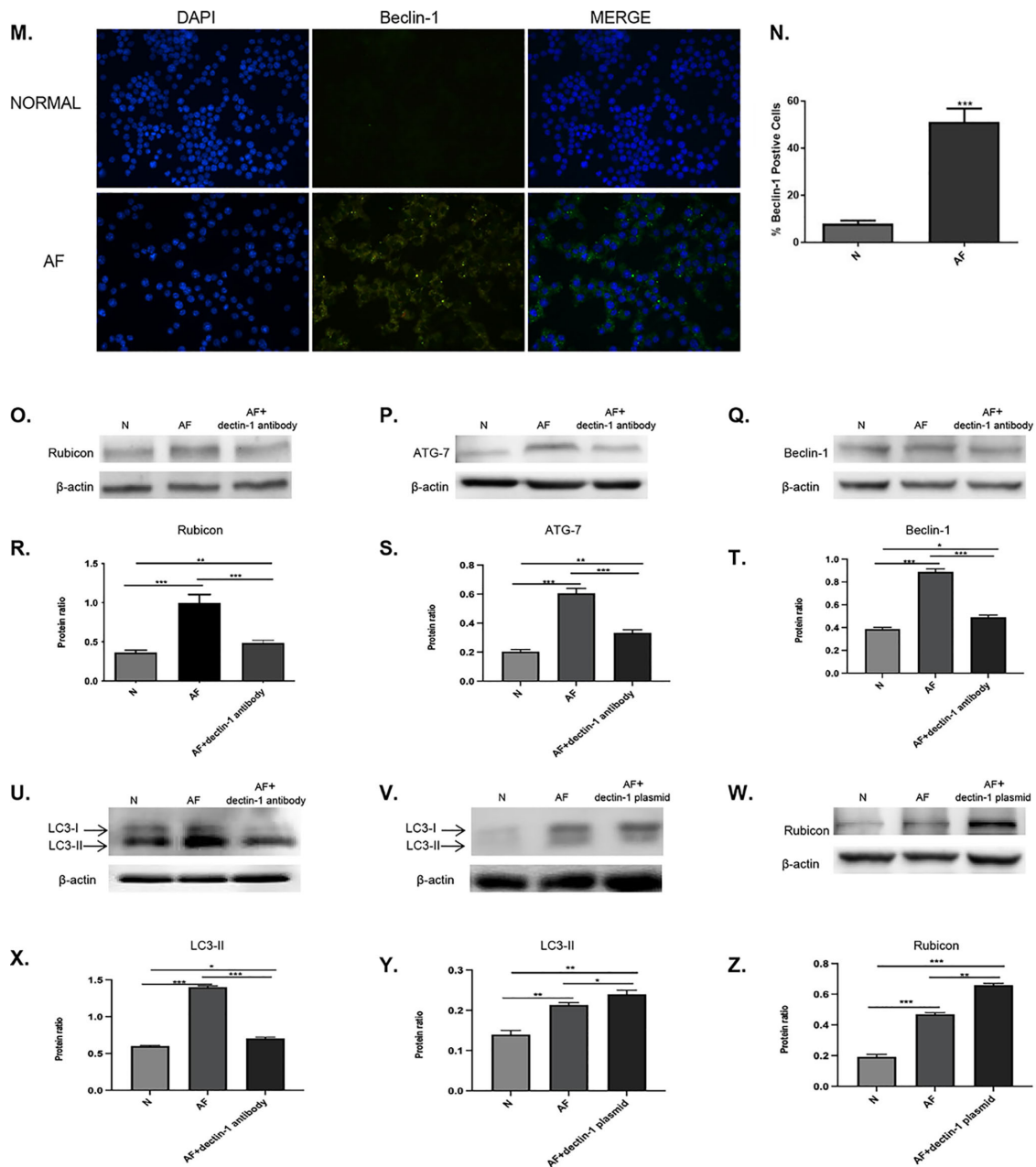


FIGURE 4. Continued.

DISCUSSION

FK is a corneal disease caused by pathogenic fungi.²⁶ In severe cases, it can lead to corneal ulcers or even corneal perforation, and may even result in loss of vision.²⁷ Recent studies have reported that LAP can enhance the efficiency of the immune response to expedite the elimination of pathogens during fungal infection.²⁰ Furthermore, studies have confirmed that LAP could play an active role in fungal infectious diseases by eliminating pathogens and reducing the inflammatory response.^{18,22} Therefore, it is crucial to explore the role of LAP in FK.

LAP is a noncanonical autophagy pathway.²⁸ Recently, research has shown that LAP plays a crucial role in the eradication of pathogenic microorganisms, such as *Candida albicans* (*C. albicans*).²⁹ In addition, Smeekens et al. found a

high recruitment of LC3-II to *C. albicans*-containing phagosomes in HeLa cells.^{29,30} Our study revealed the accumulation of single-membrane phagosomes in the macrophages of *A. fumigatus*-infected human and mice corneas, aligning with previous studies conducted in murine models of systemic lupus erythematosus (SLE).^{31,32} Our study revealed that LAP might be key participants in corneal infection induced by *A. fumigatus*.

LAP requires some conventional autophagy-related proteins, such as LC3, Beclin-1, Rubicon, etc.^{22,33} Compared with canonical autophagy, pre-initiation complex activity is not necessary for LAP, but it requires the class III PI3K complex.⁷ The class III PI3K complex member Beclin-1 is recruited to the phagosomes almost instantly.³⁴ Rubicon, a class III PI3K related protein that interacts with Beclin-1, has also been shown to be essential for the stable anchoring of

LC3-II on LAP.³⁵ Furthermore, previous studies have found that the autophagy protein ATG-7 is crucial for LAP. The absence of ATG-7 results in a reduction in the recruitment of LC3-II, which makes phagocytosis less effective in killing and eliminating apoptotic cells.¹⁶ LC3-II is localized on the monolayer membrane of phagocytic vesicles, facilitating the maturation of single-membrane phagosomes, their fusion with lysosomes, the clearance of ingested pathogens, and enhancing the efficacy of fungal elimination.^{17,34} Our results demonstrated that the expression of LAP-related proteins was significantly elevated in *A. fumigatus*-infected human and mouse corneas. Moreover, the formation of positive GFP-LC3 puncta was notably enhanced in mice corneas with FK. The above results revealed that LAP may have a potential role in *A. fumigatus* keratitis. Recent research has indicated that LAP was rapidly formed when RAW 264.7 cells phagocytosed zymosan, LPS, and *Escherichia coli*.³⁶ Consistently, stimulation with LPS upregulates the expression of LAP-associated proteins, thereby promoting the facilitation of pathogen elimination. This reminded us that LAP could play a role in the elimination of invading fungal pathogens in *A. fumigatus* keratitis. The above evidence indicated that LAP was involved in the immune process of *A. fumigatus* keratitis.

Recent research by Martinez et al. demonstrated that Rubicon functioned as a molecular switch for LAP.^{9,10} Rubicon can stabilize the class III PI3K complex to ensure that LC3-II can stably bind to single-membrane phagosomes during the LAP process, which is significant for enhancing LAPosome maturation and regulating inflammation.³⁷ Thus, we chose to intervene in the expression of Rubicon to influence the LAP process. Our study showed that si-Rubicon decreased the expression of Rubicon and LC3-II in *A. fumigatus*-infected corneas. These results indicated that si-Rubicon effectively interferes with the process of LAP, which may impact the regulatory effect of LAP on inflammation in the immune response to FK. In addition, the LAP process was completely blocked in the Rubicon^{-/-} group, leading to a higher death rate compared to the control group. Immunofluorescence analysis revealed that the expression of GFP-LC3 and other LAP-related proteins in the Rubicon^{-/-} group was significantly decreased in the *Salmonella Typhimurium* Zebrafish model.³⁸ The findings of our study demonstrated that si-Rubicon could interfere with the LAP process in *A. fumigatus* keratitis, thereby highlighting the involvement of LAP in the immune response associated with *A. fumigatus* keratitis.

Furthermore, excessive inflammation will exacerbate the tissue damage in FK.³⁹ Previous studies have shown that LAP can regulate the expression of inflammatory factors to exert anti-inflammatory effects during fungal infections.³⁵ In our study, we found that si-Rubicon treatment significantly upregulated the expression of IL-1 β and IL-6 induced by *A. fumigatus* infection, and suppressed the expression of IL-10 in *A. fumigatus*-infected corneas. Clinical scores and slit-lamp data indicate that si-Rubicon treatment significantly worsened the disease outcome. These findings indicated that interfering with Rubicon could down-regulate the LAP process and exacerbate the inflammatory response after *A. fumigatus* infected the cornea of mice. Because LAP is necessary for the efficient degradation of the engulfed corpse,²¹ when dead cells are ingested, proinflammatory cytokines are produced more frequently, and anti-inflammatory cytokines are produced less frequently.¹⁶ In our study, we revealed that LAP exhibits anti-inflammatory effects in *A. fumigatus* keratitis.

In fungal infections, the activation of Dectin-1 or TLR2 leads to the recruitment of LC3-II to phagosomal membranes.¹⁶ Dectin-1^{-/-} mice have trouble recognizing β -glucans, making them more vulnerable to *C. albicans* and *A. fumigatus* fungal infections.⁴⁰ We established the *A. fumigatus* infection model in vitro to verify the mechanism of fungal antigen-induced LAP in FK. The results showed that the expression of LAP-related proteins was upregulated in *A. fumigatus*-infected RAW264.7 cells. The treatment with the Dectin-1 antibody reduced the expression of LAP-related proteins, whereas the overexpression of the Dectin-1 plasmid increased the expression of LAP-related proteins. These data indicated that Dectin-1 may regulate the expression of LAP-related proteins in *A. fumigatus* keratitis. During infection, Dectin-1 recognizes β -glucan on the fungal cell wall.⁴¹ Previous research has demonstrated that Dectin-1 could enhance LAP by recruiting LC3 to the phagosome through spleen tyrosine kinase (Syk), thereby accelerating the fusion of LAPosomes with lysosomes.^{42,43} It has been proven that when β -glucan activates Dectin-1, the synthesis of lipidated LC3 is decreased in cells lacking Dectin-1.³⁶ Consistent with our results, Dectin-1 recognized the *A. fumigatus* that invaded the cornea, stimulated the LAP process, and induced increased expression of LAP-related proteins.⁴⁰ Our results indicated that *A. fumigatus* regulated LAP through the Dectin-1 pathway in *A. fumigatus* keratitis.

In summary, our research has identified the presence of single-membrane phagosomes in *A. fumigatus*-infected corneas for the first time and demonstrated the involvement of LAP in *A. fumigatus* keratitis. Furthermore, we have shown that LAP suppresses the expression of pro-inflammatory molecules to induce anti-inflammatory effects through the Dectin-1 pathway. From a clinical perspective, our findings open up potential therapeutic perspectives for sustaining LAP to improve the prognosis of FK. Our research findings suggest that enhancing LAP activation could serve as an effective therapeutic approach for FK. Nevertheless, the impact of LAP on modulating host immune responses seems to vary significantly based on the specific fungal species and even the strain of the fungal organism.^{44,45} Consequently, delving deeper into the molecular details of LAP is imperative to facilitate the translation of these discoveries into clinical applications.

Acknowledgments

Supported by the National Natural Science Foundation of China (No. 81870632 and 81800800), and The Taishan Scholars Program (No. ts201511108 and tsqn 201812151).

Disclosure: **J. Luan**, None; **Z. Zhang**, None; **Q. Wang**, None; **C. Li**, None; **H. Zhang**, None; **Y. Zhang**, None; **X. Peng**, None; **G. Zhao**, None; **J. Lin**, None

References

- Huang JF, Zhong J, Chen GP, et al. A hydrogel-based hybrid theranostic contact lens for fungal keratitis. *ACS Nano*. 2016;10:6464–6473.
- Fan Y, Li C, Peng X, et al. Perillaldehyde ameliorates aspergillus fumigatus keratitis by activating the Nrf2/HO-1 signaling pathway and inhibiting Dectin-1-mediated inflammation. *Invest Ophthalmol Vis Sci*. 2020;61:51.
- van de Veerdonk FL, Gresnigt MS, Romani L, et al. *Aspergillus fumigatus* morphology and dynamic host interactions. *Nat Rev Microbiol*. 2017;15:661–674.

4. Luan J, Peng X, Lin J, et al. The therapeutic potential of chondroitin sulfate in *Aspergillus fumigatus* keratitis. *Mol Immunol*. 2022;147:50–61.
5. Peng X, Zhao G, Lin J, et al. Interaction of mannose binding lectin and other pattern recognition receptors in human corneal epithelial cells during *Aspergillus fumigatus* infection. *Int Immunopharmacol*. 2018;63:161–169.
6. Mehta P, Henault J, Kolbeck R, et al. Noncanonical autophagy: one small step for LC3, one giant leap for immunity. *Curr Opin Immunol*. 2014;26:69–75.
7. Lai SC, Devenish RJ. LC3-associated phagocytosis (LAP): connections with host autophagy. *Cells*. 2012;1:396–408.
8. Sprenkeler EG, Gresnigt MS, van de Veerdonk FL. LC3-associated phagocytosis: a crucial mechanism for antifungal host defence against *Aspergillus fumigatus*. *Cell Microbiol*. 2016;18:1208–1216.
9. Martinez J, Malireddi RK, Lu Q, et al. Molecular characterization of LC3-associated phagocytosis reveals distinct roles for Rubicon, NOX2 and autophagy proteins. *Nat Cell Biol*. 2015;17:893–906.
10. Boyle KB, Rando F. Rubicon swaps autophagy for LAP. *Nat Cell Biol*. 2015;17:843–845.
11. Cemma M, Brumell JH. Interactions of pathogenic bacteria with autophagy systems. *Curr Biol*. 2012;22:R540–R545.
12. Zhong Y, Wang QJ, Li X, et al. Distinct regulation of autophagic activity by Atg14L and Rubicon associated with Beclin 1-phosphatidylinositol-3-kinase complex. *Nat Cell Biol*. 2009;11:468–476.
13. Romao S, Münz C. LC3-associated phagocytosis. *Autophagy*. 2014;10:526–528.
14. Oikonomou V, Renga G, De Luca A, et al. Autophagy and LAP in the fight against fungal infections: regulation and therapeutics. *Mediators Inflamm*. 2018;2018:6195958.
15. Martinez J. LAP it up, fuzz ball: a short history of LC3-associated phagocytosis. *Curr Opin Immunol*. 2018;55:54–61.
16. Martinez J, Almendinger J, Oberst A, et al. Microtubule-associated protein 1 light chain 3 alpha (LC3)-associated phagocytosis is required for the efficient clearance of dead cells. *Proc Natl Acad Sci U S A*. 2011;108:17396–17401.
17. Akoumianaki T, Kyrmizi I, Valsecchi I, et al. *Aspergillus* cell wall melanin blocks LC3-associated phagocytosis to promote pathogenicity. *Cell Host Microbe*. 2016;19:79–90.
18. de Luca A, Smeekens SP, Casagrande A, et al. IL-1 receptor blockade restores autophagy and reduces inflammation in chronic granulomatous disease in mice and in humans. *Proc Natl Acad Sci U S A*. 2014;111:3526–3531.
19. Huang J, Canadien V, Lam GY, et al. Activation of antibacterial autophagy by NADPH oxidases. *Proc Natl Acad Sci U S A*. 2009;106:6226–6231.
20. Tam JM, Mansour MK, Acharya M, et al. The role of autophagy-related proteins in *Candida albicans* infections. *Pathogens (Basel, Switzerland)*. 2016;5:34.
21. Kyrmizi I, Gresnigt MS, Akoumianaki T, et al. Corticosteroids block autophagy protein recruitment in *Aspergillus fumigatus* phagosomes via targeting dectin-1/Syk kinase signaling. *J Immunol*. 2013;191:1287–1299.
22. Sanjuan MA, Dillon CP, Tait SW, et al. Toll-like receptor signalling in macrophages links the autophagy pathway to phagocytosis. *Nature*. 2007;450:1253–1257.
23. Masud S, van der Burg L, Storm L, et al. Rubicon-dependent Lc3 recruitment to salmonella-containing phagosomes is a host defense mechanism triggered independently from major bacterial virulence factors. *Front Cell Infect Microbiol*. 2019;9:279.
24. Li CY, Li C, Li H, et al. Disparate expression of autophagy in corneas of C57BL/6 mice and BALB/c mice after *Aspergillus fumigatus* infection. *Int J Ophthalmol*. 2019;12:705–710.
25. Zyner KG, Simeone A, Flynn SM, et al. G-quadruplex DNA structures in human stem cells and differentiation. *Nat Commun*. 2022;13:142.
26. Lin J, He K, Zhao G, et al. Mincle inhibits neutrophils and macrophages apoptosis in *A. fumigatus* keratitis. *Int Immunopharmacol*. 2017;52:101–109.
27. Niu Y, Zhao G, Li C, et al. *Aspergillus fumigatus* Increased PAR-2 expression and elevated proinflammatory cytokines expression through the pathway of PAR-2/ERK1/2 in cornea. *Invest Ophthalmol Vis Sci*. 2018;59:166–175.
28. Wang Y, Ramos M, Jefferson M, et al. Control of infection by LC3-associated phagocytosis, CASM, and detection of raised vacuolar pH by the V-ATPase-ATG16L1 axis. *Sci Adv*. 2022;8:eabn3298.
29. Smeekens SP, Malireddi RK, Plantinga TS, et al. Autophagy is redundant for the host defense against systemic *Candida albicans* infections. *Eur J Clin Microbiol Infect Dis*. 2014;33:711–722.
30. Rosentul DC, Plantinga TS, Farcas M, et al. Role of autophagy genetic variants for the risk of *Candida* infections. *Med Mycol*. 2014;52:333–341.
31. Martinez J, Cunha LD, Park S, et al. Noncanonical autophagy inhibits the autoinflammatory, lupus-like response to dying cells. *Nature*. 2016;533:115–119.
32. Murray PJ, Allen JE, Biswas SK, et al. Macrophage activation and polarization: nomenclature and experimental guidelines. *Immunity*. 2014;41:14–20.
33. Kim JY, Zhao H, Martinez J, et al. Noncanonical autophagy promotes the visual cycle. *Cell*. 2013;154:365–376.
34. Mizushima N, Yoshimori T, Ohsumi Y. The role of Atg proteins in autophagosome formation. *Annu Rev Cell Dev Biol*. 2011;27:107–132.
35. Wong SW, Sil P, Martinez J. Rubicon: LC3-associated phagocytosis and beyond. *FEBS J*. 2018;285:1379–1388.
36. Ma J, Becker C, Lowell CA, et al. Dectin-1-triggered recruitment of light chain 3 protein to phagosomes facilitates major histocompatibility complex class II presentation of fungal-derived antigens. *J Biol Chem*. 2012;287:34149–34156.
37. Winkelstein JA, Marino MC, Johnston RB, Jr., et al. Chronic granulomatous disease. Report on a national registry of 368 patients. *Medicine*. 2000;79:155–169.
38. Kanayama M, Shinohara ML. Roles of autophagy and autophagy-related proteins in antifungal immunity. *Front Immunol*. 2016;7:47.
39. Chidambaram JD, Kannambath S, Srikanthi P, et al. Persistence of innate immune pathways in late stage human bacterial and fungal keratitis: results from a comparative transcriptome analysis. *Front Cell Infect Microbiol*. 2017;7:193.
40. Tam JM, Mansour MK, Khan NS, et al. Dectin-1-dependent LC3 recruitment to phagosomes enhances fungicidal activity in macrophages. *J Infect Dis*. 2014;210:1844–1854.
41. Werner JL, Metz AE, Horn D, et al. Requisite role for the dectin-1 beta-glucan receptor in pulmonary defense against *Aspergillus fumigatus*. *J Immunol*. 2009;182:4938–4946.
42. Ben Mkaddem S, Hayem G, Jönsson F, et al. Shifting FcγRIIA-ITAM from activation to inhibitory configuration ameliorates arthritis. *J Clin Invest*. 2014;124:3945–3959.
43. Wang Y, Sharma P, Jefferson M, et al. Non-canonical autophagy functions of ATG16L1 in epithelial cells limit lethal infection by influenza A virus. *EMBO J*. 2021;40:e105543.
44. Kanayama M, Shinohara ML. Roles of autophagy and autophagy-related proteins in antifungal immunity. *Front Immunol*. 2016;7:47.
45. Oikonomou V, Renga G, De Luca A, et al. Autophagy and LAP in the fight against fungal infections: regulation and therapeutics. *Mediators Inflamm*. 2018;2018:6195958.